

Design of a high-quality multi-terminal semiconductor switch

Juan Daniel Torres Luna

Design of a high-quality multi-terminal semiconductor switch

by

Juan Daniel Torres Luna

to obtain the degree of Master of Science
at the Delft University of Technology,
to be defended publicly on April 21st

Student number: 5213983
Project duration: August 31, 2021 – March 2, 2022
Thesis committee: Prof. Michael Wimmer, TU Delft, supervisor
Prof. Anton Akhmerov TU Delft, co-supervisor
Dr. Chun-Xiao Liu TU Delft, co-supervisor

Contents

1	Background	1
1.1	Introduction	1
1.2	Majorana bound states	2
1.3	Majorana bound states in a trijunction	3
1.4	Experimental platforms	3
1.4.1	Two dimensional electron gases	4
1.4.2	Electrostatic gates.	4
2	Trijunction of Majorana nanowires	5
2.1	Quasi-one dimensional cavities	5
2.1.1	Size dependence	6
2.1.2	Resonant trapping	7
2.2	Two dimensional cavities	7
2.2.1	Size dependence	8
2.2.2	Angular dependence	9
2.2.3	Majorana sub bands	10
3	Gate defined triangular cavities	11
3.1	Gates configuration	11
3.2	Device operation	11
3.2.1	Nanowire channels	11
3.2.2	Potential deformations.	12
4	Conclusions	13
	Bibliography	14

1

Background

1.1. Introduction

MBS appear as the zero-energy modes of a hybrid quasi-one dimensional system that combines a strong-spin orbit semiconductor with proximity induced superconductivity. Semiconducting nanowires and two-dimensional electron gases (2DEG) are candidates for creating such devices, yet no evidence of such excitations has been found. Nevertheless, the existence of MBS would allow us to design new qubits that are resilient to noise in contrast to current devices.

While coupling a single MBS pair can be done using a quantum dot, selective coupling of multiple pairs remains a challenge. In the presence of multiple pairs, coupling MBS from different fermions induces a non-trivial evolution of the ground state that supports quantum gate operation. Coupling of a pair of MBS in a S-N-S junction has been extensively studied, and the fractional Josephson effect has been found as a signature of MBS present in such system. On the other hand, coupling multiple MBS pairs remains a challenge given the constraints on the nanowires alignment and separation.

The simplest system where multiple MBS can couple non-trivially is in a trijunction geometry. *In this thesis we propose a semiconducting cavity connected to three Majorana nanowires that allows for an all-electric controlled interaction between all pairs of MBS.*

Initially, the role of geometry is investigated by simulating several cavity geometries and extracting the MBS coupling in the strong coupling regime. It is found that different cavity levels mediate differently the coupling of different MBS pairs. We found that there is an angle for a triangular cavity that induces a maximum coupling between the far MBS pairs. *Several cavity geometries are analysed, and a triangular cavity with varying angle is found to have the largest coupling for all pairs.*

Finally, a realistic model is studied via electrostatic simulations of the triangular cavity with optimal configuration defined on a 2DEG. The non-local nature of the gates makes the nanowire positions crucial in order to recover the effects found for the purely geometric case. The role of each set of gates and the range of voltages used to operate the device are discussed. *The electrostatics effects of the gate-defined triangular cavity are analysed and the operational point is described.*

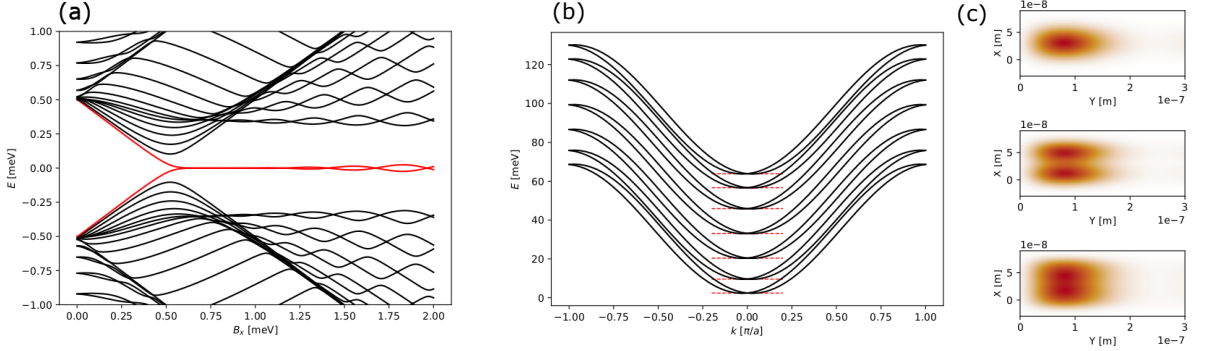


Figure 1.1: Simulations of a Majorana nanowire as described in Eq. (1.4). The following parameters will be used in all simulations: $\Delta = 0.5[\text{meV}]$, $\alpha = 0.3[\text{eV A}]$, and $t = \hbar^2/2m^*$ where $m^* = 0.023m_e$. Each simulated nanowire has length $L = 130 * a$ and width $W = 7 * a$ where $a = 10[\text{nm}]$ is the lattice constant size. (a) Topological phase transition as a function of Zeeman field B_x . Majorana zero-energy state (red) sticks to zero after crossing the critical field. (b) Transverse bands along the translational invariant direction with $\Delta = 0$. The chemical potential is tuned to the bottom of each band (red dashed lines) to create Majoranas. (c) Majorana wavefunctions for the lowest three bands.

1.2. Majorana bound states

MBS emerge as the non-local degenerate ground state of a topological superconductor. Under the appropriate conditions, a spinless one-dimensional p -wave superconductor contains two zero-energy excitations that are exponentially localised at the edges of the system. Together, these two zero-energy modes encode a single fermionic mode that can be empty or occupied,

$$f = \frac{\gamma_L + i\gamma_R}{\sqrt{2}}, \quad f^\dagger = \frac{\gamma_L - i\gamma_R}{\sqrt{2}}, \quad (1.1)$$

where $\gamma_i = \gamma_i^\dagger$ are Majorana operators that $\{\gamma_i, \gamma_j\} = 2\delta_{ij}$.

Since a pair of spatially separated MBS encode a single fermionic mode, its quantum state is protected against local errors by particle-hole symmetry. In a sufficiently large nanowire, MBS are completely decoupled from each other, and noise sources will interact with each of them individually. The interaction with a single MBS is proportional to a single Majorana operator, i.e. $\gamma \sim f + f^\dagger$, and thus it will change the parity of the system. In a superconductor, however, electrons can only enter or leave as Cooper pairs, which means that the parity is conserved. Therefore, individual MBS are immune to local noise sources.

The ground state can only be controlled by non-local operations that involve pairs of MBS. Given parity conservation, only even powers of Majorana operators are allowed in the Hamiltonian. The simplest allowed term describes the coupling of a pair of MBS, and it is given by

$$H_{pair} = iE_{LR}\gamma_L\gamma_R = E_{LR}(1 - 2f^\dagger f). \quad (1.2)$$

Here, E_{LR} is the tunnelling coupling between the two MBS, and it is usually cancelled in sufficiently long nanowires.

In the presence of multiple MBS pairs, each parity subspace can be used as a computational subspace where quantum information is protected. *By controlling the coupling between different MBS pairs, one can control the ground state evolution*, that is,

$$|\Psi\rangle \rightarrow U(t)|\Psi\rangle, \quad U(t) = \exp(iH_{pair}t). \quad (1.3)$$

1.3. Majorana bound states in a trijunction

There are two main approaches for MBS quantum computation: braiding and joint parity measurements. Braiding was initially proposed as moving MBS around each other in gate defined nanowire networks[1]. However, this method requires high degree of control and is highly susceptible to thermal errors[5]. On the other hand, joint parity measurements coupling multiple pairs of MBS[6] by using co-tunnelling processes between different MBS on superconducting islands. These methods do not rely on geometrical effects, and are often discussed in terms of a phenomenological Hamiltonian.

In a trijunction, demonstration of the simplest non-trivial Majorana evolution experiment can be done. In order to create a Majorana qubit, three or more MBS with precisely controlled interactions are required. The interaction between different MBS pairs is mediated by the cavity modes, which crucially depends on the nanowires positions and the cavity geometry. By controlling the coupling of each pair via a DC voltage pulse sequence, one determines the evolution of the MBS. Initial studies[3] have shown that MBS can connect via a semiconducting cavity in a fork-like geometry.

However, design and operation of a trijunction are non-trivial tasks. Simultaneous tuning of gate voltages and relative phase difference is required to optimally operate a trijunction. Selection of the MBS pair and cavity modes is realised by electrostatic gates controlling the potential on each region. Furthermore, relative phase differences between MBS modulates the coupling as in the fractional Josephson effect. The phase will be shifted by the presence of complex hopping terms and by the nanowires relative position.

1.4. Experimental platforms

MBS can be realised in quasi one-dimensional systems defined on two-dimensional electron gases (2DEGs), or semiconducting nanowires, with strong spin-orbit and in proximity to a superconductor. The Hamiltonian that realises a Majorana nanowire is,

$$\mathcal{H} = \sum_k \Psi_k^\dagger H(k) \Psi_k, \quad H(k) = \left[\frac{|\mathbf{k}|^2}{2m^*} - \mu + \alpha(k_x \sigma_y - k_y \sigma_x) \right] \tau_z + B_x \sigma_x + \Delta \tau_x. \quad (1.4)$$

Here, $\Psi_k^\dagger = (f_{k\uparrow}^\dagger, f_{k\downarrow}^\dagger, f_{k\uparrow} f_{k\downarrow})^T$ are the Nambu spinors in k space, μ is the chemical potential, \mathbf{k} is the 2D wave-vector, α is the spin orbit interaction, B_x is the Zeeman field, Δ is the superconducting gap, and σ and τ are Pauli matrices for the spin and particle-hole basis.

MBS appear as zero energy excitations of this Hamiltonian when $B_x^2 \geq \sqrt{\mu^2 + \Delta^2}$. However, *realising such material combination is difficult, and MBS transport signatures are not unambiguous.* On the one hand, these interaction destroy each other mutually as is the case of superconductivity and magnetic fields. On the other hand, MBS signatures can be reproduced by states localised in material defects or impurities. Therefore, highly tunable devices with low impurities and disorder are required to unambiguously detect MBS.

MBS can appear in different nanowire sub-bands. In a quasi-one dimensional systems, there is a translational invariant direction, and a direction with finite width W . The energy of each mode has a contribution from both, and it is given by,

$$E_n(k) = \frac{\hbar^2}{2m^*} \left(k^2 + \frac{\pi^2 n^2}{W^2} \right). \quad (1.5)$$

Here, m^* is the effective mass and the spin orbit splitting is not considered. Independent MBS with different momentum profiles can be formed at each transverse mode when the

chemical potential is at the bottom of the corresponding band. Multiple channel become relevant in the presence of disorder. It couples differently to each momentum sub band, which will induce band mixing as has been suggested in experiments.

1.4.1. Two dimensional electron gases

In a clean system, electrons travel ballistically, and their motion is directly determined by the shape of the system boundaries. *2DEGs allow for arbitrary geometries to be defined in the same layer using different electrostatic gates.* Furthermore, it been shown that geometric dependence can be used to enhance the property of Majorana devices. On the other hand, in semiconducting nanowires networks MBS is limited to narrow transverse channels. Therefore, 2DEGs are an interesting platform to study the role of geometry in MBS coupling with gate defined shapes.

Parallel Majorana nanowires are the basic elements for a complex Majorana device. Multiple nanowires require to be aligned in order to have a stable topological phase. Each Majorana nanowire can be defined on a 2DEG by adding a superconducting strip on top of the selected region. A a top gate is deposited next on top of the device such that depletes the surrounding 2DEG. A narrow quasi-one dimensional channel is created below the superconductor, and it is expected to find MBS at the edges.

Majorana experiments on 2DEGs have shown promising evidence for scalable and complex devices. Initial experiments[4, 7] focused on characterising the properties of semiconducting layers with a superconducting cover. Advances in material growth allowed for clean interfaces with a hard superconducting gap to develop into the nanowire region. Later experiments focused on tunnel spectroscopy of stripe-like geometries[8] where a zero bias peak (ZBP) was found. However, due to disorder and defects such ZBPs have most likely a trivial origin from Andreev states rather than MBS. Nevertheless, efforts to develop scalable devices in 2DEGs are made and new promising materials are being studied.

1.4.2. Electrostatic gates

The electrostatic potential in a 2DEG is found by solving the Poisson equation using a finite elements method on the device geometry. The potential landscape in a 2DEG can be controlled by deposition of metallic gates on a top layer with an insulating barrier in between that smooths the potential profile. The potential landscapce, $U(\mathbf{r})$, for a given geometrical configuration can be found by solving Laplace equation,

$$\nabla \cdot [\epsilon_r(\mathbf{r}) \nabla U(\mathbf{r})] = 0. \quad (1.6)$$

Here, ϵ_r is the relative permitivity of each layer in the material stack.

Electrostatic effects play a crucial role in designing and operating Majorana devices. Characterisation of Majorana nanowire is done via transport measurements that require tunnel coupled leads and gates. Furthermore, gates have a non-local effect on the potential landscape that differs between experimental platforms. For example, nanowires have a partial superconducting coating that allows for the electric field to penetrate and control the semiconductor and superconductor weight of the wavefunction. In 2DEGs, on the contrary, the superconducting coat fully covers it, which screens electrostatic effects.

2

Trijunction of Majorana nanowires

In this chapter we demonstrate that the coupling of three pairs of MBS in a trijunction is determined by the geometrical details of the central semiconducting cavity. For certain geometrical configurations, a MBS pair couples resonantly with successive cavity states as in the so-called *resonant trapping*, while in other cases the coupling is mediated by individual non-overlapping levels.

We simulate the pair coupling of three Majorana nanowires mediated by a semiconducting cavity using Kwant. For each experiment, a pair of nanowires is set to host MBS in each sub band while the other nanowire is fully depleted. We consider the strong coupling regime where there are no tunnel barriers between the cavity and the nanowires. Furthermore, the phase difference between the selected nanowires is tuned such that the coupling is at a maximum. *The coupling energy of each pair is extracted as the value of the lowest non-zero eigenvalue with respect to the cavity chemical potential.*

The cavity chemical potential is varied in a range of 4 meV around the first resonance for all cavities. In this range, there are multiple levels that couple resonantly with a given pair of MBS. *In order to characterise the coupling, we extract the highest resonance peak for each geometry.* Then, we classify them according to their operational robustness, that is, height and width.

2.1. Quasi-one dimensional cavities

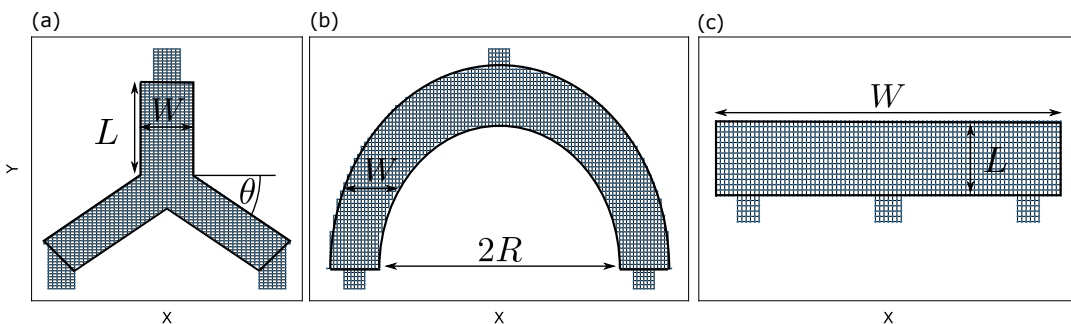


Figure 2.1: Kwant systems describing the three quasi-1D cavities: (a) Y-shaped defined by three parameters: arms length and width, L and W , and lateral arms angle θ . (b) Half-ring defined by the radius R and the width W . (c) Rectangular stripe defined by the length L and width W .

Let us start by building the simplest possible Majorana trijunction. Consider a quasi-1D cavity with mirror symmetry along the y -axis. Then, the position of the three nanowires is fixed: one is attached at the center, and one at each end. Consequently, the phase shift for the central MBS pairs is symmetric around π . Similarly, the coupling of the left-center MBS pair and center-right MBS pair is the same. Under these constraints, we study how the geometry affects the coupling of the two different pairs.

We consider three cavity geometries: In Fig. 2.1 (a) one can observe a Y-shaped cavity. In Fig. 2.1 (b) one can observe a half-ring stripe cavity with three nanowires attached in a fork-like geometry. In Fig. 2.1 (c) one can observe a rectangular stripe cavity with three Majorana nanowires attached.

It is a challenge to build a trijunction that reliably and selectively couples all three pairs of MBS. It is straightforward to couple a single MBS pair in a quasi-1D geometry since the left and right MBS pair will fully enclose the cavity wavefunctions. However, it is a challenge to create a system where the remaining two pairs can couple in a similar way.

2.1.1. Size dependence

Initially, the overall size of the system is varied, and a transition from the small to the long junction regime is found for all geometries. In Fig. 2.2 one can observe the evolution of the largest resonance peak for each geometry as a function of the system size.

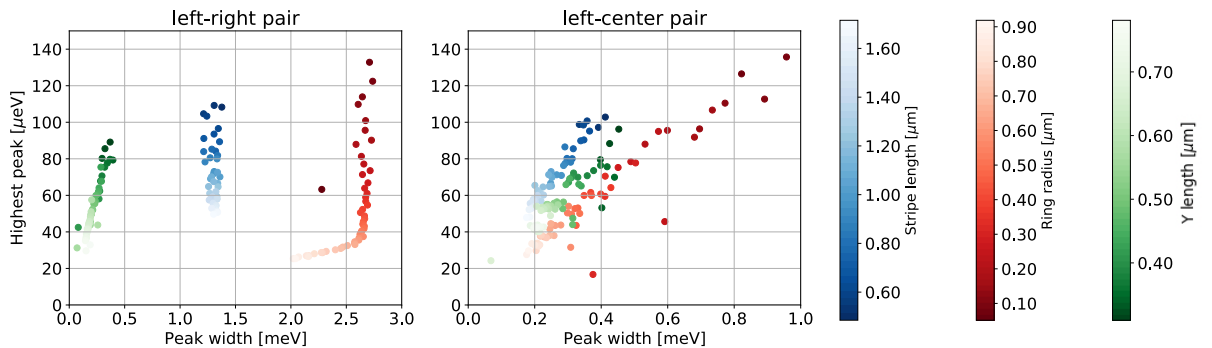


Figure 2.2: Geometrical dependence of the resonant coupling peaks for three quasi-1D geometries that correspond to each colorbar. The system was tuned to the lowest Majorana band. (a) Left-right MBS pair coupling. (b) Left-center MBS pair coupling.

The coupling of the left and right MBS pair shows a clear geometrical dependence as can be observed in Fig. 2.2 (a). Each geometry occupies a separate region in the resonant height-width plane. The ring cavity has the most robust resonant peaks. For small R , the coupling is larger than any other geometry, and it is close to $\Delta/2$. Similarly, the width is the largest, and it persists even for rings with diameter $1 \mu\text{m}$ after which decays. Then follows the stripe geometry that has approximately the same width for all considered widths. Finally, the Y-shaped cavity has overall the smallest resonant peak width.

The coupling of the central MBS pairs, on the contrary, cannot be easily separated for each geometry. Generally, one can see three diagonal stripes in Fig. 2.2 (b) where the stripe geometry has the largest resonant peak height. The peak width decreases as the size increases, and it has the same slope for all geometries. Nevertheless, for sufficiently small sizes, the ring geometry has peak heights and widths larger than any other geometry.

2.1.2. Resonant trapping

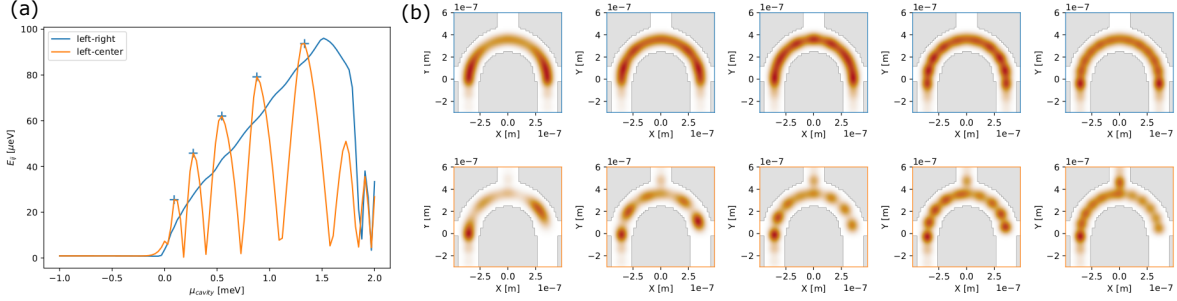


Figure 2.3: Spectra for a half-ring shaped cavity of width $W = 110$ [nm] and radius $R = 300$ [nm]. The system was tuned to the lowest Majorana band. (a) Coupling of each MBS pair. Center-right pair is the same curve as left-center pair. Crosses indicate the positions at where the wavefunction (b) are taken. The color of the frame in (b) corresponds each MBS pair in (a).

Let us consider the half-ring cavity. When the left and right nanowires are close to the ends of the cavity, the MBS pair couple along a sequence of overlapping resonant states as can be seen in the blue line of Fig. 2.3 (a). *The cavity states interfere constructively and the coupling accumulates creating a single wide peak over the resonant region.* It depends crucially on having the lead states around all of the cavity wavefunction as can be seen in Fig. 2.3 (b). This phenomena is known as *resonant trapping*.

For the central pairs coupling, in contrast, a band of resonances cannot form since the cavity wavefunction is not fully enclosed. When coupling the left and central MBS, the cavity region close to the right lead acts as a particle in a box with multiple individual levels that repel each other. Consequently, we observe the orange line shown in Fig. 2.3 (a) where the resonant band is divided in individual resonances.

The difference when coupling multiple MBS pairs relies on the geometric configuration of the cavity wavefunctions and the MBS relative positions. *Then, one can explain the distribution of couplings observed in Fig. 2.2.* The left and right MBS in the ring and stripe geometry have an approximately constant and large widths over the different system sizes because cavity levels remain resonant. On the other hand, the coupling of the central MBS pairs in any geometry has a much smaller width because some part of the wavefunction is not coupled. Particularly, the Y-shaped junction has a small width for all pairs because no resonant trajectories can be created in such geometry.

2.2. Two dimensional cavities

In a ballistic cavity, the motion of the electrons is determined by the shape of the cavity and leads. The electrons follow semiclassical trajectories connecting different leads that can be identified as peaks in the conductance. Following such intuition, we explore if changes in the geometry of a 2D cavity can be used to modulate the coupling of different MBS pairs. Particularly, we explore how the angular dependence of the incoming modes, and internal angles of the cavity, influence the MBS coupling.

We consider three geometries: In Fig. 2.4 (a) one can observe a circular cavity with Majorana nanowires attached in a fork-like geometry. In this geometry one can control the angle of the incoming MBS. In Fig. 2.4 (b) one can observe a triangular cavity with nanowires attached at the lower side. In this geometry one can control the angle of MBS

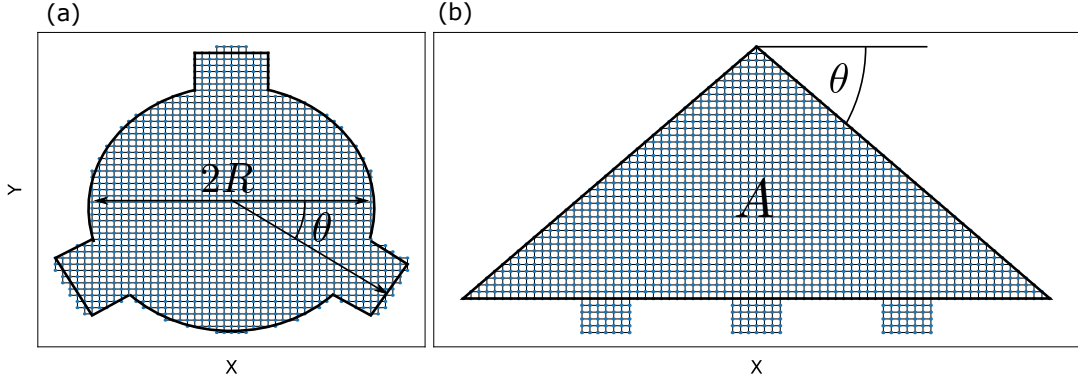


Figure 2.4: Left: Kwant system of a half-ring shaped cavity. It is defined by the radius R and the width W . Thinner rectangular segments represent the positions of the Majorana nanowires attached. Right: Lowest four eigenstates of the cavity with the nanowires fully depleted.

scattering within the cavity by changing the diagonal sides. In order to explore the role of the positioning of the leads, we explore a variation of the triangular geometry with the central lead in the top side. Lastly, we consider a rectangular geometry that can be created by extending the length of the stripe geometry shown in Fig. 2.1 (c).

2.2.1. Size dependence

Let us start by discussing the size dependence of the cavities. In Fig. 2.5 one can observe the size dependence of the resonant peak for the three two-dimensional geometries.

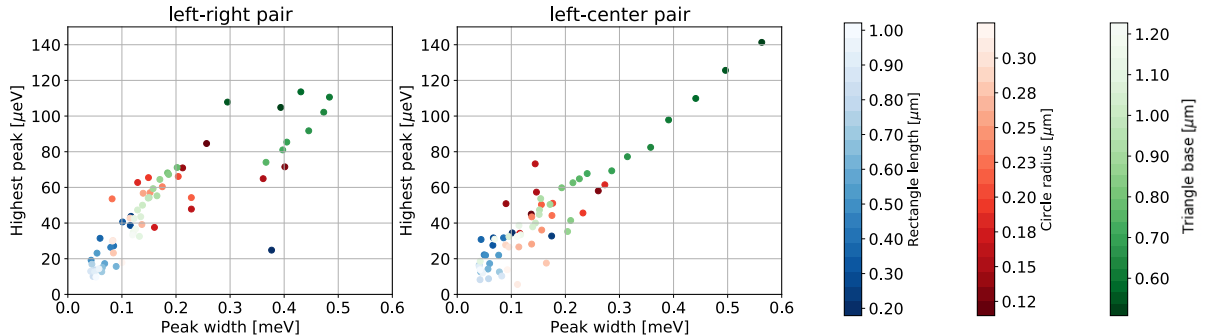


Figure 2.5: Size dependence of the three 2D geometries considered in this section corresponding to each colorbar. The system was tuned to the lowest Majorana band. The (a) left-right and (b) left-center largest resonant peaks are shown. The angle of all the cavities here is $\theta = \pi/4$.

Overall, there is no major distinction between the coupling of different pairs. All couplings decay as the system size increases following a diagonal line in panels (a) and (b). Nevertheless, the geometry dependence can be seen in three different regions along the diagonal.

On the rightmost region, one observes that the triangular geometry has the largest couplings and widths for small sizes. Descending along the diagonal, the triangular and circular geometries overlap. Remarkably, there is a significant size difference between them in the overlapping region, approximately 500 nm. Most of circular geometries are concentrated in this region. At the bottom of the diagonal, one observes that the worst MBS couplings happen for rectangular geometries.

2.2.2. Angular dependence

The angle is changed in two triangular cavities, one circular cavity, and the Y-shaped cavity. The resulting coupling for each pair and geometry is shown in Fig. 2.6.

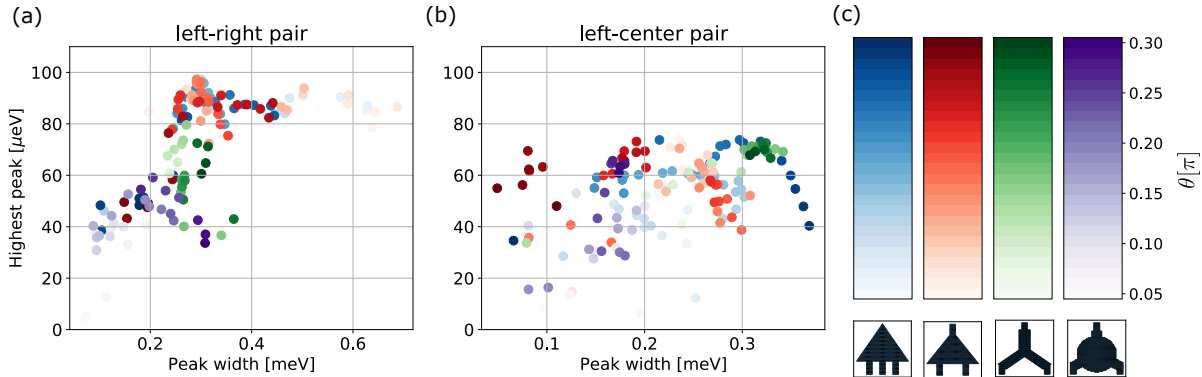


Figure 2.6: Angular dependence of the resonant coupling peaks for four geometries with angle dependence. The system was tuned to the lowest Majorana band. Each one corresponds to a colorbar as depicted in (c). (a) Left-right MBS pair coupling. (b) Left-center MBS pair coupling. The area of the triangular cavities was $A = 900 [a^2]$. The radius of the circular cavity is $R = 250 [\text{nm}]$. The size of the Y-shaped cavity is similar to that of the triangular cavity.

The triangular geometry shows a transition from the resonant trapping regime to the single resonance regime while maintaining an approximately constant peak height. One can observe that the peak height stays around the same value for a large range of angles in panel (a). This behaviour is present in both triangular geometries since the red and blue dots highly overlap. The width, on the other hand, is inversely proportional to the angle. For small angles, the width is the largest for 2D geometries, around 0.7 meV. As the angle increase, the width decreases until it saturates around 0.3 meV.

In order to understand this behaviour, let us observe that for small angles the triangular cavity resembles a quasi-1D system. By cutting the edges of the stripe geometry, the wavefunction is concentrated towards the center such that it can be easily trapped between the left and right leads as observed in the blue curve of Fig. 2.7 (a). As the angle increases, the resonant band splits into several sub bands that contain a few resonances each as observed in Fig. 2.7 (b). If the angle increases further, these resonances fully split into individual levels, thus explaining the saturation found in Fig. 2.6 (a).

The coupling of the left and central MBS pair -on the contrary- is more complicated to analyse due to the high overlap between geometries as observed in Fig. 2.6 (b). Couplings for both triangular geometries are around the same region in width and height for small angles. As the angle increases, the width of the configuration with central lead at the lower side (blue) increases, while the other configuration (red) decreases.

It is remarkable that the triangular geometry has two configurations that can be used to operate a Majorana trijunction with similar coupling magnitude and width for all MBS pairs. These two configurations are shown in Fig. 2.7. Note, however, that the small angle configuration would be rather considered a quasi-1D system since the ration between its dimensions. That is the reason why the resonant band has such a large width and encloses many states. Nevertheless, resonant trapping is still present in the second configuration, but with fewer states inside the resonant band.

For the remaining geometries, there is indeed a modulation for the left and right MBS

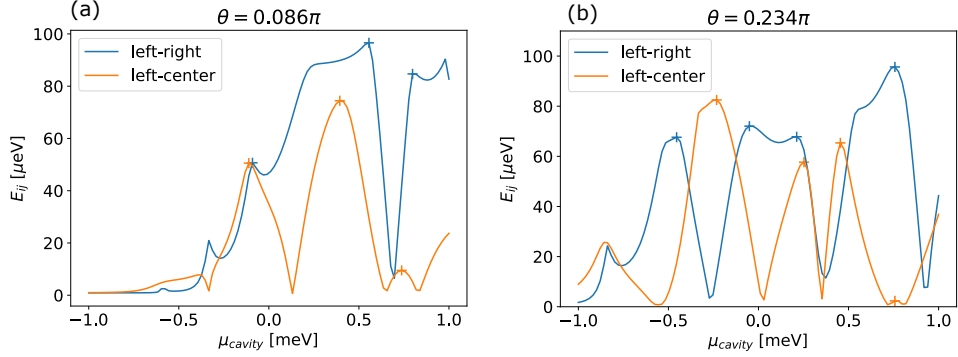


Figure 2.7: Coupling of triangular geometries with the central lead at the (a) top and (b) bottom sides. The total area of the triangle is $A = 1200 [\text{a}^2]$.

pairs. However, the overall coupling remains smaller and narrower than the triangular case. Interestingly, the left and central MBS coupling for the Y-shaped cavity converges to a region around $(0.3\text{meV}, 70\mu\text{eV})$ as the angle increases (see Fig. 2.6 (b) green points). On the other hand, the behaviour of this pair in the circular cavity does not show a clear trend.

2.2.3. Majorana sub bands

By tuning each nanowire sub band into the topological phase, we probe the momentum distribution of the cavity states. In Fig. 2.8 one can observe the mean coupling for each band. It has been averaged over all geometrical configurations and all MBS pairs since no clear distinction between them was found.

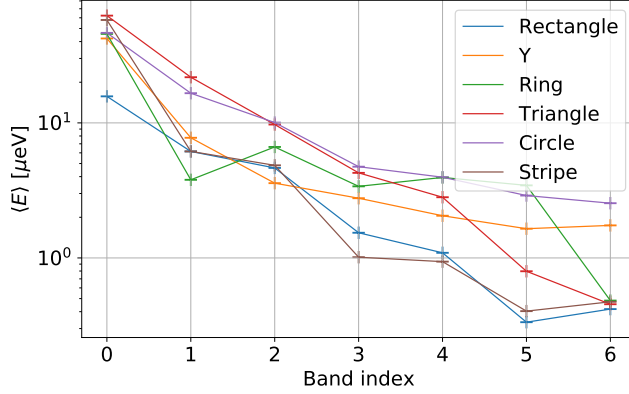


Figure 2.8: Mean geometry-pair coupling for all Majorana sub band and all geometries considered in this section. The geometry average was taken over the data shown in Fig. 2.5.

Overall, the coupling decays exponentially as the band index increases. The decay is modulated by the geometry, but the trend holds in all cases. There is, approximately, two order of magnitude decrease in the coupling from the lowest to the highest band.

The lowest band carries the largest coupling. This allows us to infer that the momentum distribution of cavity states is dominated by low momentum states. This is reasonable since the coupling of spatially separated MBS requires delocalised cavity states. However, a precise quantitative description of the momentum profiles inside the cavity goes beyond the scope of this work.

3

Gate defined triangular cavities

In the previous chapter we have found that the best geometries to couple MBS are the ring and the triangular geometries. The coupling of different pairs is highly asymmetric in the ring geometry, while it is similar in the triangular geometry. Then, we consider that a triangular trijunction is more reliable when selectively coupling multiple MBS pairs.

3.1. Gates configuration

1. The triangular cavity is defined using electrostatic gates, and the potential in the 2DEG is found as the solution to the Poisson equation.
2. It is not clear if the geometric dependence holds in a real device where the boundaries of the system are not straight, but smooth following the potential landscape.
3. In contrast to a purely geometric model, changing a single gate has a non-local effect that affects other regions of the potential, possibly inducing unexpected behaviours.
4. The MBS coupling depends on the tradeoff between tunability and shape-resolution determined crucially by the position where the nanowires attach to the cavity.
5. Consider a material stack made by an InAs 2DEG with proximity induced superconductivity, and a set of metallic gates with an oxide layer in between.
6. There are three kinds of gates in this system: plunger gates and screen gates that control the shape of the cavity, and tunnel gates that control the coupling with the nanowires.
7. Devices with three nanowires at one side are larger than those with two because of the minimum separation between tunnel barriers which is required to have well defined coupling channels for each nanowire.

3.2. Device operation

3.2.1. Nanowire channels

1. In order to have the minimum number of tunnable gates, each nanowire requires a tunnel barrier well separated from each other by fixed-voltage screen gates.

2. The operation point is below the first barrier level resonance in order to avoid interaction with spurious levels and keep a clean cavity dependence.
3. By controlling the tunnel gates height relative to the nanowire's potential, the tunnelling amplitude can be changed from the insulating regime to the strong coupling regime.
4. When the tunnel gates are far from each other, there is no crossed interaction between them, and they can be tuned symmetrically.
5. For closer tunnel gates, there's mutual interaction that modifies the barrier height, center and width, leading to a non-symmetric operational point.

3.2.2. Potential deformations

1. While the left and right MBS coupling is optimal for a triangular cavity, the coupling of the central pairs is significantly smaller due to the large system size.
2. The triangular shape of the cavity is controlled by three gates, the plunger and the screen side gates, and can be deformed in order to probe modified shapes with increased couplings.
3. The coupling of the central pairs can be significantly increased by detuning the side screen gates and effectively creating smaller triangular cavities.
4. Potential deformations are not allowed in a geometry with the central wire attached to the top triangle vertex because the screen gates determine both the cavity shape and the barrier's positions.
5. Similarly, a configuration with nanowires attached to the diagonal sides would induce irregularities along these sides that would significantly decrease the MBS coupling.

4

Conclusions

1. Triangular cavities show a maximum coupling for a certain angle for the far pair, while the coupling of the central pair can be tuned to a maximum or minimum depending on the wire's side.
2. In a gate defined cavity, the position of the nanowires plays a crucial role in the definition and tunability of the triangular shape and thus enhancing or decreasing the MBS coupling.
3. A natural extension of this work is to design an experiment where joint parity measurements can be measured via interferometry in a loop geometry, or via charge measurements with a nearby sensor.
4. Another possible extension is to include realistic noise, representing the etching process, as potential irregularities along the triangle sides.
5. In conclusion, a trijunction of MBS where the coupling of all pairs is comparable to the superconducting gap has been designed and the operation of the device has been discussed in terms of electrostatic gates.

Bibliography

- [1] J. Alicea, Y. Oreg, G. Refael, F. V. Oppen, and M. P. Fisher. Non-abelian statistics and topological quantum information processing in 1d wire networks. *Nature Physics*, 7:412–417, 2011.
- [2] P. Bonderson, M. Freedman, and C. Nayak. Measurement-only topological quantum computation. 2 2008.
- [3] M. Hell, J. Danon, K. Flensberg, and M. Leijnse. Time scales for majorana manipulation using coulomb blockade in gate-controlled superconducting nanowires. *Physical Review B*, 94:1–32, 2016.
- [4] M. Kjaergaard, F. Nichele, H. J. Suominen, M. P. Nowak, M. Wimmer, A. R. Akhmerov, J. A. Folk, K. Flensberg, J. Shabani, C. J. Palmstrom, and C. M. Marcus. Quantized conductance doubling and hard gap in a two-dimensional semiconductor-superconductor heterostructure. 3 2016.
- [5] F. L. Pedrocchi and D. P. DiVincenzo. Majorana braiding with thermal noise. *Physical Review Letters*, 115:1–6, 2015.
- [6] S. Plugge, A. Rasmussen, R. Egger, and K. Flensberg. Majorana box qubits. *New Journal of Physics*, 19, 2017.
- [7] J. Shabani, M. Kjaergaard, H. J. Suominen, Y. Kim, F. Nichele, K. Pakrouski, T. Stankevic, R. M. Lutchyn, P. Krogstrup, R. Feidenhans'l, S. Kraemer, C. Nayak, M. Troyer, C. M. Marcus, and C. J. Palmstrøm. Two-dimensional epitaxial superconductor-semiconductor heterostructures: A platform for topological superconducting networks. 11 2015.
- [8] H. J. Suominen, M. Kjaergaard, A. R. Hamilton, J. Shabani, C. J. Palmstrøm, C. M. Marcus, and F. Nichele. Zero-energy modes from coalescing andreev states in a two-dimensional semiconductor-superconductor hybrid platform. 3 2017.
- [9] L. Wirtz, J. Z. Tang, and J. Burgdörfer. Geometry-dependent scattering through ballistic microstructures: Semiclassical theory beyond the stationary-phase approximation. *Physical Review B - Condensed Matter and Materials Physics*, 56:7589–7597, 1997.